



# Multi-Objective Optimization as a Tool for Material Design

Zahed Allahyari and Artem R. Oganov

## Contents

1	Introduction	2
2	What Is the Pareto Front?	2
3	Different MO Methods	4
3.1	Layer Classification (A Simple Pareto Ranking)	4
3.2	Vector Evaluated Genetic Algorithm (VEGA) (Schaffer 1985)	5
3.3	Non-dominated Sorting Genetic Algorithm (NSGA)	5
3.4	Pareto Envelope-Based Selection Algorithm (PESA)	6
3.5	Strength Pareto Evolutionary Algorithm (SPEA)	6
4	Combining MO Optimization with USPEX for Material Design	8
4.1	Example 1: $\text{Mo}_x\text{N}_y$	10
4.2	Example 2: $\text{Fe}_x\text{B}_y$	11
4.3	Example 3: $\text{Mo}_x\text{B}_y$	11
5	Conclusion	13
	References	13

---

Z. Allahyari (✉)

Materials science and Engineering, Skolkovo Institute of Science and Technology,  
Moscow, Russia

Moscow Institute of Physics and Technology, Moscow, Russia

e-mail: [zahed.allahyari@gmail.com](mailto:zahed.allahyari@gmail.com)

A. R. Oganov

Materials science and Engineering, Skolkovo Institute of Science and Technology,  
Moscow, Russia

Moscow Institute of Physics and Technology, Moscow, Russia

International Center for Materials Design, Northwestern Polytechnical University, Xi'an, China

e-mail: [a.oganov@skoltech.ru](mailto:a.oganov@skoltech.ru)

---

**Abstract**

In this chapter, we explain the concept of Pareto optimality and Pareto dominance and use these concepts in solving multi-objective (MO) optimization problems. Then, we discuss a few different MO optimization methods and show how MO optimization can be used as a tool for designing new materials. A simple Pareto-based MO optimization method is examined on a few practical case studies to assess how efficient is this method in optimizing double-objective problems.

---

## 1 Introduction

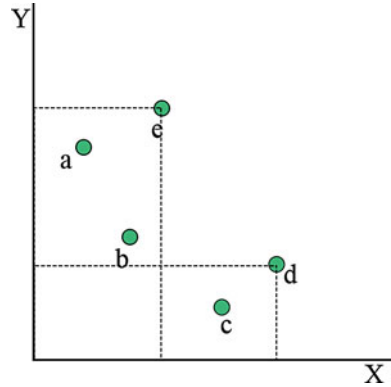
In today's world, computational optimization is essential for solving the problems in a wide area of scientific, technological, and engineering applications. Generally, these problems can be classified into single-objective (SO) and multi-objective (MO) problems. SO problems are problems with only one objective to be optimized. But MO problems are problems with more than one objectives which have to be optimized simultaneously. MO optimization is usually more complex than SO, since instead of a single objective, several, often conflicting objectives need to be optimized. This means that improving one objective usually ends up in degrading the other objectives. In MO problems there is a set of optimal solutions which is called Pareto front. The task of MO optimization methods is to find this optimal set of solutions, so that a decision-maker can then select solutions preferable from various considerations (e.g., cost, or expected ease of synthesis, etc.). Optimizing energy alone gives one the stable phase, which usually (but not always) is easy to synthesize, but does not necessarily possess the best properties. Optimizing physical properties alone gives the theoretical limit for the property of interest – but the predicted phase may be so high in energy that its chances to be synthesizable are negligible. MO optimization, simultaneously optimizing energy and the property of interest, is the best way known to us to find solutions that are practically interesting, possessing attractive properties and with a high chance (albeit not a guarantee) of being synthesizable. In this chapter, it is shown that how MO optimization methods can be useful in solving the central problem of computational material design, which is the discovery of new materials optimal in multiple properties; therefore, at first, several different MO optimization methods are discussed and it is shown how MO optimization can be used as a tool for designing new materials. Then, a simple Pareto-based MO optimization method is applied to a few practical cases, demonstrating the efficiency of this method in optimizing double-objective problems.

---

## 2 What Is the Pareto Front?

The goal of MO optimization methods is to find the set of optimal solutions with a trade-off between the objectives. This set of solutions is called Pareto front. To understand how the Pareto front is obtained, the concept of dominance is useful.

**Fig. 1** Illustration of dominance concept



Pareto dominance, Pareto optimality, and Pareto front are the concepts that are commonly used for comparison of candidate solutions in a population. A solution **a** is said to dominate solution **b**, if **a** is at least as good as **b** in every objective and better than **b** in at least one objective. Figure 1 is a schematic representation of solutions on the Ashby plot (Ashby 2011) (Ashby plot is a two-dimensional plot of any two objectives where each objective is plotted along one of the axes of the plot). The goal in this illustration is to find the set of solutions that minimize X and Y objectives in the best way. In this figure, solution **c** dominates solution **d**, because **c** has lower (or better) value of both objectives than **d**. **a** and **b** dominate **e** for the same reason. But **a**, **b**, and **c** do not dominate each other. For example, **a** is better than **b** and **c** in one objective, while it is worse than them in the other objective. Solutions **a**, **b**, and **c** that are not dominated by any other solutions are said to be non-dominated solutions. In fact, Pareto front is a set of non-dominated solutions.

In mathematical terms, for a set of solutions  $\{S_n\}$  ( $n = 1, \dots, N$ ), each solution with  $F_m$  ( $m = 1, \dots, M$ ) objectives, MO optimization can be formulated as follows:

```

S = [S1, S2, ... SN];           # The set of solutions,
F = [F1, F2, ... FM];           # The set of objectives,
counter = 0;
Pcounter = ∅;
while length({S}) ≠ 0           # While there are solutions in
                                the population.
    S = (S ∪ Pcounter) - (S ∩ Pcounter) # Removing the non-
                                        dominated solutions
                                        # from population
    Si dominates Sj, (i, j = 1, ..., N and i ≠ j)
    If Fk(Si) ≤ Fk(Sj) (k = 1, ..., M), for all objectives
        and
        Fk(Si) < Fk(Sj), At least in one objective
    S* = Si if Si is not dominated by any other solutions
    counter = counter + 1;
    {Pcounter} = S* # copying non-dominated solutions to {P}
end

```

A solution  $S^*$  is not dominated by any other and is, therefore, Pareto optimal.  $\{P_t\}$  ( $t = 1, \dots, T$  and  $T \leq N$ ) is a set of non-dominated solutions. After finding the set of non-dominated solutions,  $\{P_1\}$  or first Pareto front, these solutions are removed from the main population, and again the non-dominated solutions of the rest of the population are found – these form the second Pareto front,  $\{P_2\}$ . This process is continued until all solutions are classified in different Pareto fronts. In the worst situation, that each Pareto front only includes one solution,  $T$  can be equal to  $N$ . This usually happens when objectives are not conflicting, i.e., a linear relation exists between all objectives.

In MO optimization, if one solution can be found which is more optimal than all other solutions in every objective, it is called Utopian solution. For single objectives, there is always a utopian solution, while generally there is no utopian solution for MO problems.

---

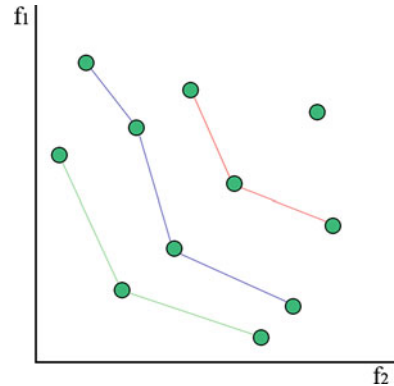
### 3 Different MO Methods

For designing an efficient Pareto-based MO optimization method, generally, two important factors need to be optimized. The distance to the optimal front is to be minimized, and the diversity of the generated solutions is to be maximized. The latter is useful when more than two objectives are optimized. In the following, we discuss simple Pareto ranking method which is already sufficient for double-objective optimization as well as a few more complex methods in MO optimization.

#### 3.1 Layer Classification (A Simple Pareto Ranking)

The set of non-dominated solutions (solutions forming the Pareto front) are determined using dominance concept. These are the most optimal solutions in the current population, thus the best rank (highest probability of selection) is assigned to this set of solutions. Then these solutions are eliminated from the population temporarily, and again, Pareto front for the rest of population is found. This procedure is repeated until all solutions are classified into different Pareto fronts (Fig. 2). To all the solutions of the same Pareto front, the same fitness is assigned, and there is no priority in selecting the structures of the same Pareto front. Obviously, the highest probability of selection is given to the solution of the first Pareto front, the second highest probability to the second Pareto front, and so on. Then the selection can be performed using any binary selection method (like tournament selection). We call this method “layer classification Pareto technique.” Some of the methods that are introduced in this chapter are using this layer classification technique. However, since this method fails in some cases particularly when the number of objectives increases, all of the following methods use some additional technique to make sure that successful results are accessible even if the number of objectives increases.

**Fig. 2** Layer classification of solutions in different Pareto fronts for minimizing both objectives



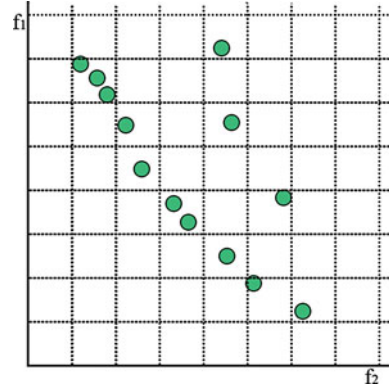
### 3.2 Vector Evaluated Genetic Algorithm (VEGA) (Schaffer 1985)

This method is not based on Pareto optimality techniques. This method works as a typical genetic algorithm with one difference, which applies in the way of parent selection method. Let us assume an  $m$ -objective problem with  $N$ , number of best fraction of solutions in each generation that are allowed to be selected as a parent. At the end of each generation, the population is ranked for each single objective, and the  $N/m$  of best ranked solutions is added to a hypothetical archive. In this way, if a solution is optimal in  $n$  objectives ( $n \leq m$ ), it is  $n$  times more likely to be selected than a solution optimal in only one objective. However, this method is susceptible to the shape of the Pareto front, and it fails to generate solutions which do not necessarily excel in one objective but optimal in a sense of Pareto front (Ngatchou et al. 2005).

### 3.3 Non-dominated Sorting Genetic Algorithm (NSGA)

In the proposed NSGA (Srinivas and Deb 1994), a layer classification method is used, and a sharing function is then applied to the solutions of each Pareto front in the way that some priorities are given to the solutions in the less crowded regions. This sharing function is totally dependent on the choice of sharing parameter,  $\delta_{share}$ , which is a user-predefined parameter. This parameter denotes the largest value of distance metric within which two solutions share each other's fitness (Deb et al. 2002). But because of the user dependencies and other failures of this fitness sharing method (for more details please refer to reference (Srinivas and Deb 1994)), it was replaced with "crowded-comparison approach" in NSGA-II (Deb et al. 2002) to overcome the failures of fitness sharing method. This approach again gives some priorities to the solutions placed in the less crowded regions of each Pareto front, while it has no user-dependent parameter.

**Fig. 3** Illustration of selection method in PESA



### 3.4 Pareto Envelope-Based Selection Algorithm (PESA)

In this method, only the non-dominated solutions (Pareto front solutions) are permitted to be ranked and selected. Here, after determining the Pareto front, a hypervolume is defined as a result of finding the closest distance of two neighbor solutions for each objective. This hypervolume estimates the isolation factor for solutions in the way that each solution in a hypervolume with the maximum number of solutions gets the minimum isolation value and vice versa (Fig. 3). The probability of selection of these solutions is proportion to their isolation value. The goal is to give a higher probability to the solutions in the isolated regions than those in the crowded regions. This way of selecting individuals – based on the probability which is given to each of them – is called “individual-based selection.” But this method was replaced with “region-based selection” in PESA2. In the region-based selection, instead of giving an isolation value to each individual, the isolation value is given to hypervolumes, and as a result, selection is applied on hypervolumes instead of solutions. This way, the hypervolume which contains less solutions is considered to be more isolated than the one with more solutions (hypervolumes with higher isolation values are preferred). After selection of a hypervolume, one of its solutions is chosen randomly. This method is shown to be more efficient and preferred by the author (Corne et al. 2001) than individual-based selection. For more details on distribution of probabilities and selection mechanism, we refer to the original paper (Corne et al. 2001).

### 3.5 Strength Pareto Evolutionary Algorithm (SPEA)

Like NSGA and PESA, there are two versions for SPEA, the first version was published on 1999 (Zitzler and Thiele 1999), but later it turned out that this method has serious problems in special situations and was claimed in some works (Corne et al. 2001; Zitzler et al. 2001; Deb et al. 2002) to be unsuccessful in finding the optimal solution. However, in SPEA2 (2001) (Zitzler et al. 2001), the selective

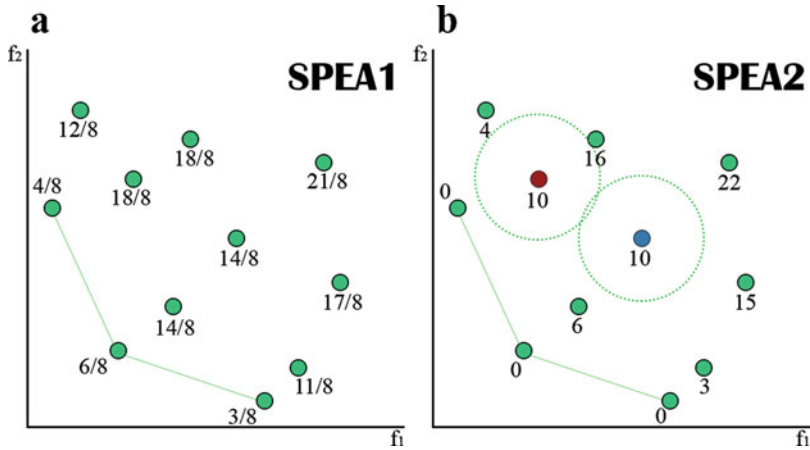


**Fig. 4** Different fitness assignment in (a) SPEA1 and (b) SPEA2 for the same distribution of solutions. According to the density estimation technique which is used in SPEA2, the blue solution has the higher chance of being selected than the red one, since it is placed in the less crowded region

fitness assignment method was totally changed, and a more solid algorithm was proposed. Here, we discuss the way of fitness assignment in both methods and briefly mention the main failures of SPEA1.

**SPEA1:** In this method (Zitzler and Thiele 1999), the population is divided into two groups, *external* (non-dominated solutions) and *internal* (dominated solutions). In SPEA1 optimal solutions can be selected from both external and internal population; hence, fitness is assigned to all population members. This fitness is evaluated using a predefined strength function. For a non-dominated solution (in external population), strength is equal to the number of other solutions it dominates, divided by  $N$ , in which  $N$  is the size of internal population. For a dominated solution (in the internal population), strength is obtained by summing up the strength of non-dominated individuals that dominate it, divided by  $N$ . The selective fitness is equal to the strength of the solution if the solution is a member of external population. Otherwise, selective fitness is equal to the strength of solution plus one (to make sure non-dominated solutions are always preferred to dominated solutions) (Fig. 4a). However, the method fails when many solutions are dominated by the same non-dominated individuals (and consequently, they all have the same fitness). For example, in the particular case that only one non-dominated solution exists, SPEA behaves like a random search algorithm. Moreover, SPEA is mostly unsuccessful in convergence/quick convergence to the optimal solutions.

**SPEA2:** For the sake of eliminating the deficiencies of SPEA, SPEA2 method was proposed (Zitzler et al. 2001). In fact, the fitness assignment in this method totally differs from the previous version. In SPEA2, for improving the convergence rate to the best optimal solutions, an archive with a fixed size is defined in which only the solutions of this archive are allowed to be selected. If the number

of non-dominated solutions fits the archive's size, then only these solutions are selected. But if the number of non-dominated solutions exceeds the archive's size, non-dominated solutions from the dense regions (regions containing many non-dominated solutions in each other's vicinity) are eliminated from the archive. For more details on density estimation technique which is used in SPEA2, we refer to the original paper (Zitzler et al. 2001). In the case that the size of archive is larger than the number of non-dominated solutions, free places will be filled by dominated solutions according to their fitness (in the case of same fitness value for many solutions, density estimation technique is used).

**Fitness assignment:** At first, strength is computed for each solution (both dominated and non-dominated), which is equal to the number of other solutions it dominates. Then, a raw fitness is defined which is obtained by summing up the strength of solutions (both dominated and non-dominated) that are dominating the target individual (therefore, raw fitness is zero for all non-dominated individuals). Then a fitness is assigned to each individual, which is equal to the sum of raw fitness and the density of the region (in the case of the same raw fitness for two or more solutions). It must be mentioned that in both SPEA1 and SPEA2, the fitness is to be minimized. Although SPEA2 was claimed to be very effective in MO optimization, it can be clearly seen from Fig. 4b that this algorithm fails in some cases to give a proper ranking to the non-dominated solutions, i.e., the blue solution has better ranking than the red one (because it is placed in a less crowded region), while the red solution belongs to the second Pareto front and blue solution to the third Pareto front.

---

## 4 Combining MO Optimization with USPEX for Material Design

We performed MO evolutionary search for materials optimal in two properties: hardness and stability (energy above convex hull), for a few binary systems, i.e.,  $\text{Fe}_x\text{B}_y$ ,  $\text{Mo}_x\text{B}_y$ , and  $\text{Mo}_x\text{N}_y$ , using the USPEX code (Oganov and Glass 2006; Lyakhov et al. 2013). In these calculations, the simple Pareto ranking method (layer classification Pareto technique) without any further procedures such as fitness sharing, crowded comparison, clustering or any other methods (to consider the density of solutions in the objective space) was used. The reason for this choice is these additional procedures strengthen the MO Pareto-based methods when three or more objectives are under study. Although they can be also useful when dealing with two objectives, it is better to keep it simple as long as it works very well (this method was efficiently used in the prediction of new hard (Kvashnin et al. 2017) and thermoelectric (Núñez-Valdez et al. 2016) materials).

In this method, at the end of each evolutionary generation, a fitness is assigned to each structure, and fitness is derived from the Pareto rank of the structure. Thus, the highest rank (lowest fitness) will be assigned to the structures forming the first Pareto front, and these structures have the highest probability of being selected as parents. Then structures of the next generation will be created by applying



variation operators (heredity and mutation) to these parents. One can expect that the combination of MO optimization and evolutionary search should be very effective. The main reason of this effectiveness is that the method always tries to fill the blank places in the Ashby plot in which structures with multi-optimal properties must be placed. These places are filled by creating new structures that were produced by optimum parent structures chosen from the same region of the Ashby plot. Since an unlimited number of structures can be created, and only optimum structures have a chance to be selected (bad structures are discarded from the population instantly), the blank places of Ashby plot will be filled as long as there are good structures in reality to be placed there (this method is also useful when a divergent Pareto front is obtained). Of course, finding all optimum structures of these regions may need long time and even then is not guaranteed. However, by taking advantage of this well-defined method which intelligently produces optimal solutions, even in a limited time and computations power, useful (even if approximate) Pareto fronts are obtained.

It is worth mentioning that the method of MO optimization discussed here is effective for minimum multidimensionality (two dimensions), and the efficiency decreases dramatically when the number of objectives (properties to be studied for each material) increases. This is obviously due to the increase of the number of optimal structures. The dimensionality of Pareto front is proportional to the number of properties that we wish to optimize. For example, when the dimensionality increases from two to three, the Pareto front is not a line (one-dimensional) anymore. It becomes a plane (two-dimensional). Similarly, for four properties, the Pareto front becomes a 3D hyperplane and so on. Thus, the number of optimal structures which are placed on the Pareto front increases (all having the same highest rank), and the intelligent evolutionary algorithm turns to a useless algorithm with a random parent selection.

In the following, a few examples of crystal structure prediction using evolutionary methodology USPEX in combination with simple Pareto ranking (layer classification) method is given. The goal of these calculations is to find hard and stable structures in target systems using MO optimization method and assess the efficiency of this method along with evolutionary crystal structure prediction. In these examples, all the ab initio calculations were done using the PBE exchange-correlation functional (Perdew et al. 1996) and the projector-augmented wave (PAW) method (Blöchl 1994; Kresse and Joubert 1999), as implemented in the VASP code (Kresse and Furthmüller 1996) with the plane-wave basis set cutoff of 550 eV and Brillouin zone sampling using a grid of spacing  $2\pi \times 0.06 \text{ \AA}^{-1}$ . Evolutionary calculations for each binary system had initial population size = 120 and subsequent population size of 60 structures and were run for 50 generations. Hardnesses were computed using the Lyakhov-Oganov model (Lyakhov and Oganov 2011).

## 4.1 Example 1: $\text{Mo}_x\text{N}_y$

Since stable compounds of  $\text{Mo}_x\text{N}_y$  system were previously studied (Yu et al. 2016) using SO optimization mode of USPEX, this is a very good example which gives a chance to compare results and consequently realize how efficient is the simplest MO optimization method which is implemented in USPEX.

In the previous work (Yu et al. 2016),  $\text{MoN}$ ,  $\text{MoN}_2$ , and  $\text{Mo}_4\text{N}_3$  were the stable compounds under zero pressure. Also, two very low-energy metastable structures for  $\text{Mo}_2\text{N}$  and one metastable structure for  $\text{Mo}_3\text{N}_2$  were reported (Yu et al. 2016). However, in our search, the results are a little bit different. We found four stable compounds ( $\text{MoN}$ ,  $\text{MoN}_2$ ,  $\text{Mo}_2\text{N}$ , and  $\text{Mo}_3\text{N}_2$ ) for this system. The reason for this difference is that in our search, the stable structure of  $\text{Mo}_4\text{N}_3$  has not been found, and as a consequence, metastable structures of  $\text{Mo}_2\text{N}$  and  $\text{Mo}_3\text{N}_2$  appeared on the convex hull (Fig. 5a). Although  $\text{Mo}_4\text{N}_3$  was not found in our search, all other stable and metastable compounds, which were reported in the previous work, were found. Moreover, a new metastable compound ( $\text{Mo}_5\text{N}_2$ ) with energy of 2 meV/atom above the convex hull was discovered in our calculation, which has never been reported before. Also, we found another structure for  $\text{Mo}_2\text{N}$  with the  $Cmcm$  space group that is a little more stable than the computationally predicted  $I4_1/amd$  structure (Yu et al. 2016) of this compound. It is worth mentioning that the stable  $P6_3/mmc$ - $\text{MoN}_2$  structure that was found in our work is in perfect agreement with the stable structure computationally reported for  $\text{MoN}_2$  (Yu et al. 2016) and is lower in energy by 0.8 eV/atom (thus, thermodynamically more stable) than the experimentally reported (but later shown by Yu et al. (2016) to be incorrect)  $R\bar{3}m$  structure.

Altogether, this example shows that MO optimization not only discovered a few unknown low-energy metastable structures but also successfully reported all already studied stable and metastable structures of  $\text{Mo}_x\text{N}_y$  system (except one,  $\text{Mo}_4\text{N}_3$ ).

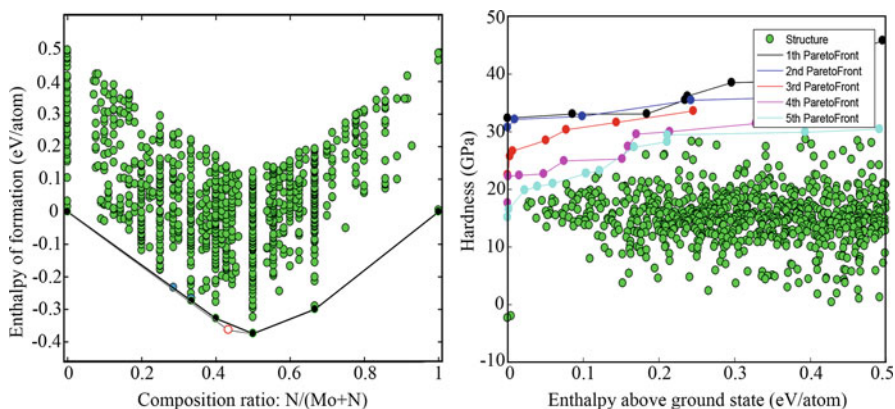


**Fig. 5** Convex hull diagram (left) and Ashby plot of hardness and energy above the convex hull (right) for the Mo-N system. The red hollow circle shows the stable  $\text{Mo}_4\text{N}_3$  compound reported in the literature. Low-energy metastable  $\text{Mo}_5\text{N}_2$  and  $Cmcm$  structure of  $\text{Mo}_2\text{N}$  are colored in blue

This indicates that MO optimization method (in the case of optimization of two properties) is almost as efficient as SO optimization.

Figure 5b shows the Ashby plot of hardness and instability of  $\text{Mo}_x\text{N}_y$  system. It can be seen from this figure that several hard and stable/low-energy metastable structures were found in this system. Although most of the structures in this figure are in the hardness range of 10–20 GPa and energy range of 0.1–0.5 eV/atom above the convex hull, it can be clearly seen that the algorithm has tried to focus on the regions where optimal structures in both properties are located.

## 4.2 Example 2: $\text{Fe}_x\text{B}_y$

In the second example, we study the  $\text{Fe}_x\text{B}_y$  system using the same method. For this system two stable binary compounds ( $\text{FeB}$  and  $\text{FeB}_3$ ) and several metastable compounds ( $\text{FeB}_2$ ,  $\text{FeB}_3$ ,  $\text{FeB}_4$ ,  $\text{Fe}_2\text{B}$ ,  $\text{Fe}_3\text{B}_5$ , and  $\text{Fe}_3\text{B}_{10}$ ) were found in our work. Some of these compounds were reported to be stable or metastable in the literature (Kolmogorov et al. 2010; Van Der Geest and Kolmogorov 2014), while some are discovered in our work. Below we discuss the differences between our results and reported findings.

In the literature,  $\text{FeB}$ ,  $\text{FeB}_2$ , and  $\text{Fe}_2\text{B}$  are discussed to be stable, while  $\text{Fe}_2\text{B}$  and  $\text{FeB}_2$  turned out to be metastable in our calculation, by 3 meV/atom and 42 meV/atom, respectively. Even though both of these compounds were found in our search, the lowest-energy structures of these compounds still have not been found. The other difference is that two structures of  $\text{FeB}_3$  were found in our calculation. Most likely, this compound would not appear on the convex hull if the stable structure of  $\text{FeB}_2$  was found; nevertheless,  $\text{FeB}_3$  is not reported neither as a stable nor as a metastable compound in the literature.  $\text{FeB}_4$  was found to be metastable in our work, which is in agreement with the literature (Kolmogorov et al. 2010; Van Der Geest and Kolmogorov 2014).  $\text{Fe}_4\text{B}$  is one of the reported metastable compounds that have not been detected in our calculation. In this calculation, several simultaneously hard and stable/low-energy metastable phases were detected for this system, and some of these are superhard (Fig. 6b).

## 4.3 Example 3: $\text{Mo}_x\text{B}_y$

$\text{Mo}_x\text{B}_y$  system is the third example in our list. For this system,  $\text{MoB}$  and  $\text{MoB}_2$  were found to be stable, which is fully in agreement with the literature (Spear and Liao 1988; Liang et al. 2012). In addition to these stable compounds, many metastable compounds were reported both theoretically (Zhang et al. 2010) and experimentally (Spear and Liao 1988) in the literature, i.e.,  $\text{MoB}_3$ ,  $\text{MoB}_4$ ,  $\text{Mo}_2\text{B}$ ,  $\text{Mo}_2\text{B}_5$ ,  $\text{Mo}_3\text{B}_2$ , and  $\text{Mo}_5\text{B}_3$ . In our search, we found eight low-energy metastable compounds ( $\text{Mo}_2\text{B}$ ,  $\text{MoB}_3$ ,  $\text{MoB}_5$ ,  $\text{Mo}_3\text{B}_5$ ,  $\text{Mo}_3\text{B}_2$ ,  $\text{Mo}_4\text{B}$ ,  $\text{Mo}_5\text{B}_2$ , and  $\text{Mo}_2\text{B}_3$ ), three of them are already reported metastable compounds ( $\text{Mo}_2\text{B}$ ,  $\text{Mo}_3\text{B}_2$ , and  $\text{MoB}_3$ ), and five of them,  $\text{MoB}_5$ ,  $\text{Mo}_2\text{B}_3$ ,  $\text{Mo}_3\text{B}_5$ ,  $\text{Mo}_4\text{B}$ , and  $\text{Mo}_5\text{B}_2$ , with the

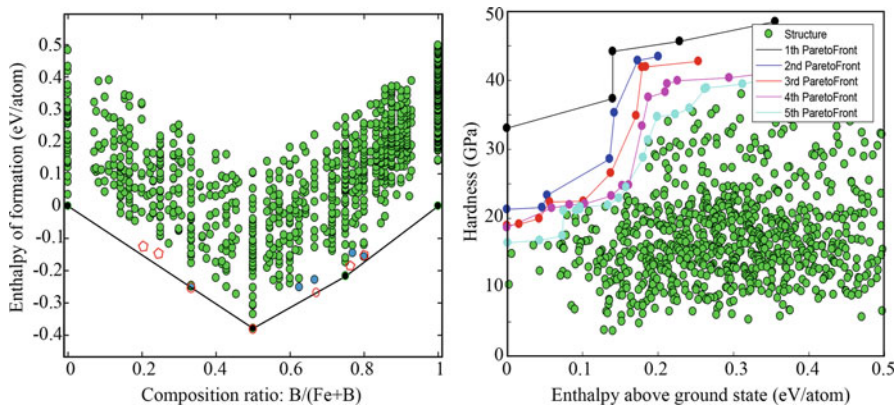


**Fig. 6** Convex hull diagram (left) and Ashby plot of hardness and energy above the convex hull (right) for the Fe-B system. The red hollow circles and polygons show the stable and metastable compounds reported in the literature. Low-energy metastable structures found in our work are colored in blue

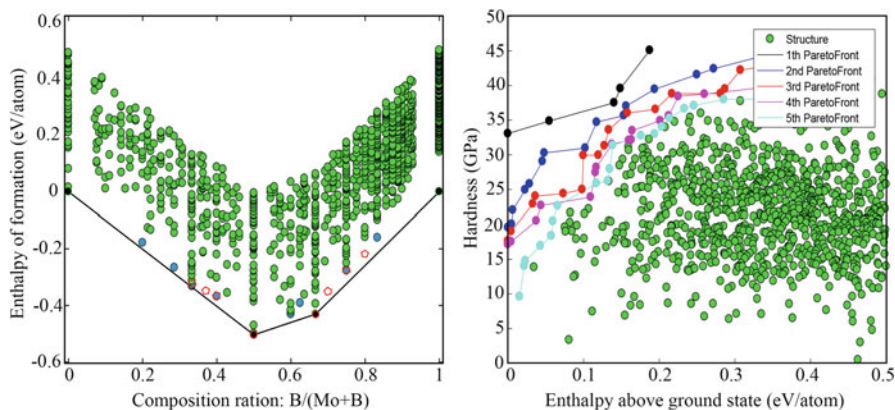


**Fig. 7** Convex hull diagram (left) and Ashby plot of hardness and energy above the convex hull (right) of the Mo-B system. The red hollow polygons show the metastable compounds reported in the literature, while blue circles indicate the compounds discovered in our work

55 meV/atom, 29 meV/atom, 57 meV/atom, 23 meV/atom, and 21 meV/atom energy above the convex hull, respectively, are unknown compounds which are discovered in our work. Although three reported metastable compounds ( $\text{MoB}_4$ ,  $\text{Mo}_2\text{B}_5$ , and  $\text{Mo}_5\text{B}_3$ ) have not been found in our calculation, the MO optimization acted successfully by discovering five new low-energy metastable compounds of  $\text{Mo}_x\text{B}_y$  system, which indicates the efficiency of the method in crystal structure prediction with multi-optimal properties. In Figs. 6b and 7b, the hardest stable compound (with the hardness of 33.6 GPa) corresponds to pure  $\alpha$ -boron.

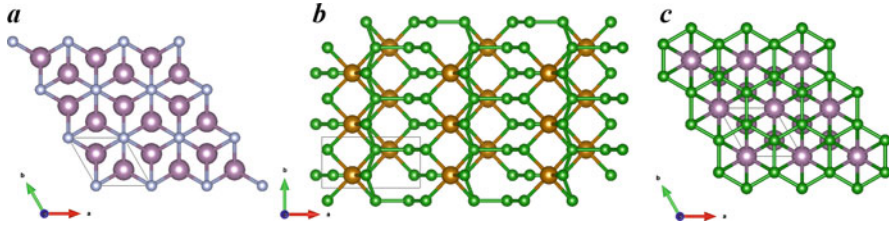


**Fig. 8** Structures of stable binary compounds with the highest Lyakhov-Oganov hardness in the systems considered here: (a)  $P6_3/mmc$ -MoN2 (Chen's hardness 22.3 GPa), (b)  $P2_1/m$ -FeB3 (Chen's hardness 30.2 GPa), (c)  $R-3m$ -MoB2 (Chen's hardness 28.5 GPa)

Stable binary compounds with the highest Lyakhov-Oganov hardness for each of the above examples are MoN2 (32.6 GPa), FeB3 (20 GPa), and MoB2 (19.6 GPa). These phases have space groups  $P6_3/mmc$ ,  $P2_1/m$ , and  $R-3m$ , respectively, and are shown in Fig. 8. While Lyakhov-Oganov model of hardness is convenient for screening (it is very cheap and numerically robust), more accurate values are predicted using Chen's model (Chen et al. 2011) – the latter, however, requires calculations of the elastic tensor and is therefore much more computationally expensive and is sensitive to numerics. Thus, after initial screening, the final hardnesses were computed using Chen's model.

## 5 Conclusion

In this chapter, some of the most prominent multi-objective optimization methods were discussed, and the “layer classification” Pareto technique in combination with USPEX was used in search for simultaneously hard and stable materials. The most realistic and favorable outcome of material design is the discovery of new materials with simultaneously optimal multiple properties; i.e., in our examples, unstable hard materials are as useless as soft stable materials. We need to have materials which are optimal in all required properties. Therefore, MO optimization method can be used as a verified tool for materials discovery. Searching for materials with optimal multi-properties is possible using the combination of evolutionary search and MO Pareto ranking. The combination of these two provides a powerful tool for the search and discovery of new materials.

**Acknowledgments** We thank the Russian Science Foundation (grant 16-13-10459) and the “5 top 100” program of MIPT for the financial support.

## References

- Ashby MF (2011) Materials selection in mechanical design. Butterworth-Heinemann, Burlington  
 Blöchl PE (1994) Projector augmented-wave method. Phys Rev B 50:17953–17979. <https://doi.org/10.1103/PhysRevB.50.17953>

- Chen X-Q, Niu H, Li D, Li Y (2011) Modeling hardness of polycrystalline materials and bulk metallic glasses. *Intermetallics* 19:1275–1281. <https://doi.org/10.1016/J.INTERMET.2011.03.026>
- Come D, Jerram N, Knowles JD et al (2001) PESA-II: region-based selection in evolutionary multiobjective optimization. In: Proceedings of the genetic and evolutionary computation conference, pp 283–290. doi: citeulike-article-id:8133801
- Deb K, Pratap A, Agarwal S, Meyarivan T (2002) A fast and elitist multiobjective genetic algorithm: NSGA-II. *IEEE Trans Evol Comput* 6:182–197. <https://doi.org/10.1109/4235.996017>
- Kolmogorov AN, Shah S, Margine ER et al (2010) New superconducting and semiconducting Fe-B compounds predicted with an *Ab Initio* evolutionary search. *Phys Rev Lett* 105:217003. <https://doi.org/10.1103/PhysRevLett.105.217003>
- Kresse G, Furthmüller J (1996) Efficient iterative schemes for ab initio total-energy calculations using a plane-wave basis set. *Phys Rev B* 54:11169–11186. <https://doi.org/10.1103/PhysRevB.54.11169>
- Kresse G, Joubert D (1999) From ultrasoft pseudopotentials to the projector augmented-wave method. *Phys Rev B* 59:1758–1775. <https://doi.org/10.1103/PhysRevB.59.1758>
- Kvashnin AG, Oganov AR, Samtsevich AI, Allahyari Z (2017) Computational search for novel hard chromium-based materials. *J Phys Chem Lett* 8:755–764. <https://doi.org/10.1021/acs.jpcclett.6b02821>
- Liang Y, Yuan X, Fu Z et al (2012) An unusual variation of stability and hardness in molybdenum borides. *Appl Phys Lett* 101:1–6. <https://doi.org/10.1063/1.4764547>
- Lyakhov AO, Oganov AR (2011) Evolutionary search for superhard materials: methodology and applications to forms of carbon and TiO<sub>2</sub>. *Phys Rev B* 84:92103. <https://doi.org/10.1103/PhysRevB.84.092103>
- Lyakhov AO, Oganov AR, Stokes HT, Zhu Q (2013) New developments in evolutionary structure prediction algorithm USPEX. *Comput Phys Commun* 184:1172–1182. <https://doi.org/10.1016/j.cpc.2012.12.009>
- Ngatchou P, Zarei A, El-Sharkawi A (2005) Pareto multi objective optimization. In: Proceeding of the 13th international conference on, intelligent systems application to power systems, pp 84–91. <https://doi.org/10.1109/ISAP.2005.1599245>
- Núñez-Valdez M, Allahyari Z, Fan T, Oganov AR (2016) Efficient technique for computational design of thermoelectric materials. *Comput Phys Commun* 222:152–157. <https://doi.org/10.1016/j.cpc.2017.10.001>
- Oganov AR, Glass CW (2006) Crystal structure prediction using ab initio evolutionary techniques: principles and applications. *J Chem Phys* 124:244704. <https://doi.org/10.1063/1.2210932>
- Perdew JP, Burke K, Ernzerhof M (1996) Generalized gradient approximation made simple. *Phys Rev Lett* 77:3865–3868. <https://doi.org/10.1103/PhysRevLett.77.3865>
- Schaffer JD (1985) Multiple objective optimization with vector evaluated genetic algorithms. In: 1st International conference on genetic algorithms, pp 93–100
- Spear KE, Liao PK (1988) The B–Mo (Boron-Molybdenum) system. *Bull Alloy Phase Diagr* 9:457–466. <https://doi.org/10.1007/BF02881867>
- Srinivas N, Deb K (1994) Multiobjective optimization using nondominated sorting in genetic algorithms. *Evol Comput* 2:221–248. <https://doi.org/10.1017/CBO9781107415324.004>
- Van Der Geest AG, Kolmogorov AN (2014) CALPHAD: computer coupling of phase diagrams and thermochemistry stability of 41 metal – boron systems at 0 GPa and 30 GPa from first principles. 46:184–204. <https://doi.org/10.1016/j.calphad.2014.03.005>
- Yu S, Huang B, Jia X et al (2016) Exploring the real ground-state structures of molybdenum dinitride. *J Phys Chem C* 120:11060–11067. <https://doi.org/10.1021/acs.jpcc.6b00665>
- Zhang M, Wang HH, Wang HH et al (2010) Structural modifications and mechanical properties of molybdenum borides from first principles. *J Phys Chem C* 114:6722–6725. <https://doi.org/10.1021/jp100225c>

- 
- Zitzler E, Thiele L (1999) Multiobjective evolutionary algorithms: a comparative case study and the strength Pareto approach. *IEEE Trans Evol Comput* 3:257–271. <https://doi.org/10.1109/4235.797969>
- Zitzler E, Laumanns M, Thiele L (2001) SPEA2: improving the strength pareto evolutionary algorithm. *Evolutionary methods for design optimization and control with applications to industrial problem*, pp 95–100. <https://doi.org/10.3929/ethz-a-004284029>